



HAL
open science

A viscoplastic model including damage for argillaceous rocks

Mountaka Souley, K. Su, Gilles Armand, Mehdi Ghoreychi

► **To cite this version:**

Mountaka Souley, K. Su, Gilles Armand, Mehdi Ghoreychi. A viscoplastic model including damage for argillaceous rocks. 1. International Symposium on computational geomechanics (COMGEO 2009), Apr 2009, Juan-les-Pins, France. pp.146-157. ineris-00973339

HAL Id: ineris-00973339

<https://ineris.hal.science/ineris-00973339>

Submitted on 4 Apr 2014

HAL is a multi-disciplinary open access archive for the deposit and dissemination of scientific research documents, whether they are published or not. The documents may come from teaching and research institutions in France or abroad, or from public or private research centers.

L'archive ouverte pluridisciplinaire **HAL**, est destinée au dépôt et à la diffusion de documents scientifiques de niveau recherche, publiés ou non, émanant des établissements d'enseignement et de recherche français ou étrangers, des laboratoires publics ou privés.

A VISCOPLASTIC MODEL INCLUDING DAMAGE FOR ARGILLACEOUS ROCKS

M. Souley

Institut national de l'environnement industriel et des risques, Nancy, France

K. Su

Agence nationale de gestion des déchets radioactifs, France. Currently at Total, Pau, France

G. Armand

Agence nationale de gestion des déchets radioactifs, Bure, France

M. Ghoreychi

Institut national de l'environnement industriel et des risques, Verneuil, France

ABSTRACT: *Based on numerous studies of laboratory tests and in-situ observations, a macroscopic viscoplastic model which aims to improve the viscoplastic strain prediction within the Excavated Damaged Zone (EDZ) is proposed by introducing a damage variable in Lemaître's model parameters. The main characteristics of the model are: (a) the short-term behaviour is based on a generalized Hoek-Brown model, damage in the pre-peak phase is described by plasticity theory; (b) the long-term behaviour is based on the modified Lemaître's model, the changes in viscoplastic strain rates due to damage are taken into account by varying the creep activation energy and the strain-hardening parameter as a function of the current damage rate. The proposed model is implemented in the code FLAC^{3D}. Simulations of triaxial compression tests at different levels of confining pressure provide a verification of the implemented model. The influence of damage on the creep behaviour was highlighted by simulating: (a) a multi-stage creep test and by comparing the viscoplastic deformation according to whether the sample remains intact or damaged; (b) a 1-D cylindrical cavity excavated in a viscoplastic medium subjected to an isotropic stress state.*

1 INTRODUCTION

In order to demonstrate the feasibility of a radioactive waste repository in claystone formations, the French national radioactive waste management agency (ANDRA) started in 2000 to build an underground research laboratory (LS/MHM) at Bure (near the boundary between the Meuse and Haute-Marne departments) located about 300 km east of Paris. The host formation consists of a claystone (Callovo-Oxfordian argillites) and lies between 420 m and 550 m deep. Numerous programmes of laboratory tests (uniaxial/triaxial, mono/multi-stage creep and relaxation) have been undertaken for characterizing mechanical and hydromechanical short-term and long-term behaviour of these argillites. These programmes consist of more than 300 tests carried out by 4 different laboratories.

The main features of the short-term mechanical behaviour observed in the samples of argillites can be summarized as: (a) a linear behaviour under low deviatoric stresses. In triaxial compression, the loss of linearity of stress-lateral strain curves begins approximately at 50 % of the peak deviatoric stress; (b) an appearance of plastic strains at low deviatoric stress; (c) for low confining pressures, the failure of the samples is brittle and can be idealized by formation of a shear band inclined with respect to sample axis. Under high confining pressure, the mechanical behaviour is ductile.

The experimental study of creep made it possible to characterize the long-term behaviour with regard to the confining pressure, mineralogical variability and saturation. The main features of the viscoplastic response can be summarized as follows: (a) the effect of loading rate on the argillite strength is low and remains in the same order of magnitude as that of mineralogical variability; (b) the relaxation tests showed: (i) the stabilization of the deviatoric stress a few days after loading; (ii) the existence of a threshold below which the viscoplastic behaviour is not activated; (c) from creep tests, simultaneous measurement of axial and lateral strains shows that volumetric strains are negligible; (d) in the phase corresponding to the secondary creep for long term tests, the creep strain rate increases non-linearly with the applied deviatoric stresses ranging between 5 and 15 MPa. Moreover, the creep strain rates slowly decrease with time.

On the basis of these observations, several constitutive models for short as well as long term behaviour were developed for Meuse/Haute-Marne argillites, in the framework of MODEX-REP European project (Su, 2003). For the short-term behaviour, the majority of these models are elastoplastic type with strain hardening/softening and taking into account the damage through the theory of plasticity or damage mechanics. Some of these models are hydro-mechanically coupled under saturated and/or unsaturated conditions. As a result, a constitutive model based on Hoek and Brown criterion has been used by ANDRA for *in-situ* experiment design purposes (Su 2003, Souley et al. 2003). In this generalized Hoek-Brown model, damage in the pre-peak phase is described by the theory of plasticity and the transition between brittle failure and ductile behaviour, as observed in the laboratory investigations, is also incorporated.

For long-term behaviour, several teams involved in the project agree on the modified Lemaître's model without creep threshold. Certain authors (Miehe et al. 2003 in Su 2003) proposed an elasto-viscoplastic model with instantaneous plasticity (say, a unification of both short-term and long-term behaviour) without coupling between the instantaneous plasticity and viscoplasticity. Consequently, the viscoplastic behaviour in the post-failure range is exactly the same than that of intact material and the failure criterion is not affected by the rate of loading. This does not seem to be consistent with the high viscoplastic strain rates obtained in some creep tests at high deviatoric stresses close to the failure. On the other hand, in their works on unification between the two responses of argillites (short-term and long-term), Shao et al. (2003) or more recently Zhou et al. (2008) assume that the time-dependent degradation due the long-term behaviour affects both elastic modulus and failure surface.

Moreover, more than 400 m horizontal galleries at the main level of -490 m at LS/MHM laboratory have been instrumented since April 2005. The continuous measurements of convergences of the galleries are available contributing to better understanding of the time-dependent response of the argillites at natural scale. Analysis of convergence data over a period of 2 years leads to the following conclusions: (a) viscoplastic strains are anisotropic and depend on the gallery orientation with regard to the initial stress anisotropy in the investigated formation; (b) the viscoplastic strain rates observed in the undamaged area far from the gallery walls are of the same order of magnitude as those obtained in samples, whereas those recorded in the damaged or fractured zone near to the walls are one to two orders of magnitude higher; indicating the damage influence on viscoplastic strains.

Based on these observations, a macroscopic viscoplastic model which aims to improve the viscoplastic strain prediction in the EDZ is proposed by introducing damage variable in Lemaître's model. The main characteristics of the model are: (a) the short-term behaviour is based on a generalized Hoek-Brown model; (b) the long-term behaviour is based on the modified Lemaître's model, the changes of viscoplastic strain rates due to damage are taken into account by varying the creep activation energy and the strain-hardening as a function of the current damage rate. The proposed model is implemented in FLAC^{3D}. In order to verify

both constitutive equations and their implementations, several simulations are performed: (a) triaxial tests at different confining pressures; (b) single- and multi-stage creep tests; (c) relaxation tests with different total axial strain levels etc.. Finally, two 1-D simulations (with and without damage effect on viscoplastic strains) were made on a cylindrical cavity in a rock mass subjected to an isotropic stress state providing the first examples of practical applications.

2 DATA FROM IN SITU MEASUREMENTS

During the excavation works convergence measurements sections and radial extensometers have been emplaced to follow drift deformations. The following chapter depicts some of the typical measurements taken in drift at the main level of the URL.

2.1 Experimental set up

Fig. 1 shows the typical set up installed in situ, mainly in the drifts parallel or perpendicular to the major horizontal stress (Wileveau et al., 2006). Two instrumented arrays for convergence and displacement measurements have been put in place very close to the front face (around 1.5 meters) in order to investigate deformation as a function of excavation steps and time. The arrays are composed of radial extensometers, for which the end point, at 20 m far from the wall, is considered as a fixed point, and convergence sections.

The convergence has been measured manually using a system of invar wire in between 6 anchor points.

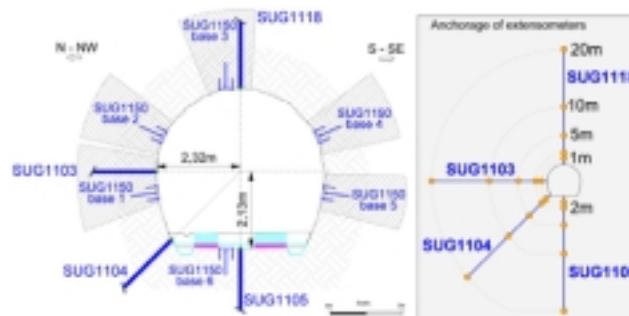


Fig. 1. Convergence measurements and extensometers in section SMR1.1

2.2 Drift deformation

Convergence of drift has been measured at different locations during the excavation work and after excavation. Fig. 2 shows the examples of measurements (vertical and horizontal) performed in different sections in the drifts parallel to σ_h . The vertical convergence exhibits huge differences. After 3 years, vertical convergence amplitude can change up to a ratio of 1.4. It is important to notice that section SUG1150 and SUG1160 are one meter apart from each other. Horizontal convergences do not show such a heterogeneity.

Armand et al. (2009) presented the average evolution of convergence in drifts parallel or perpendicular to the major horizontal stress. Obviously, the behaviour in both drift directions is very different and strongly linked to the in situ stress anisotropy. In the drifts parallel to σ_H , evolutions of vertical and horizontal convergences are very similar. The horizontal convergence is slightly higher than the vertical one. The convergence rate, 3 years after the excavation, is 0.008 mm/day. In the drifts perpendicular to the horizontal major stress, the vertical convergence is much higher than the horizontal one. It could be noticed that the horizontal convergence measured in drift parallel to σ_h is also smaller than that observed in the drift parallel to σ_H (nearly 4 times smaller). Three years after the excavation, vertical

convergence rate is 0.023 mm/day (3 times higher than the convergence rate measured in a perpendicular drift).

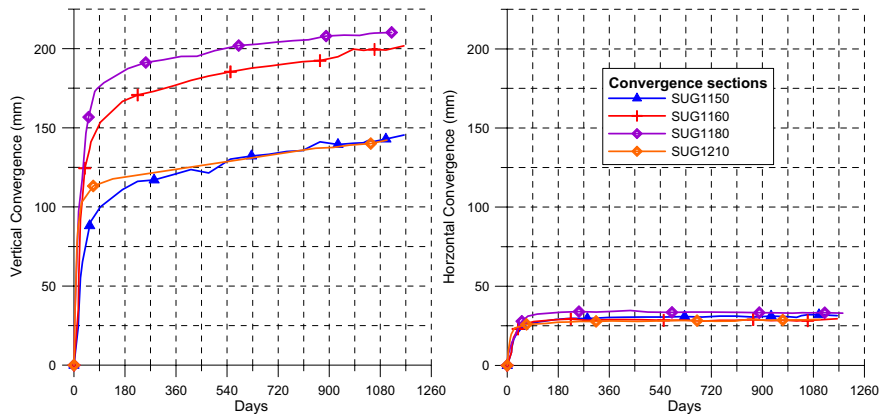


Fig.2 Examples of vertical and horizontal convergences measured in drift parallel to σ_h

The measurements also show that high convergence rates are correlated with the fracture extent. Description of the fracture pattern observed at the main level, with shear fractures (herringbone fractures and sub vertical fractures) and extension fractures, could be found in Armand et al. (2007) and Armand et al. (2009). The convergence amplitudes are in good agreement with fractures extent. For example, in the drift parallel to σ_h , significant convergence is observed between floor and vault where the fracture zone reaches nearly 2 m (plastic deformation).

The extensometers give the opportunity to better locate the high deformation rate in the vicinity of the drifts. Deformation has been calculated in between the different anchors of vertical and horizontal extensometers at SMR1.1. Figs. 3 & 4 show the evolution of deformation as a function of time. The extensometer has been emplaced on 17th August 2005 at PM32.5, the excavation resumed on 19th August 2005, and was finalized on 28th September 2005, at PM49.6 (meaning 17 m away from the extensometer section). The deformations increased a lot during the first 3 months (after the extensometer emplacement) even if the excavation work has been accomplished for 40 days. The most significant deformation reaches nearly 2% and occurs between 1 and 2 m from the wall where the highest density of fractures has been observed by coring the wall (Fig. 3). Between the wall and 1 m from the wall, the deformation remains important.

On the horizontal extensometer (Fig.4), the maximal deformation is less than 0.2% (10 times lower the one measured at the vault). The higher deformations are measured in the first meter from the wall where fractures have been observed on drilled core. Between 1 m and 2 m from the wall, deformations are in compression since the beginning, what need to be explained (it could be an artefact due to the extensometer). Deformation measurements exhibit that the highest deformation and the deformation rate are localized in the fractures zone.

Convergence and extensometer measurements suggest the effect of the fractured zone on the deformation, meaning that rock mass behaviour is not representative of that of the fractured.

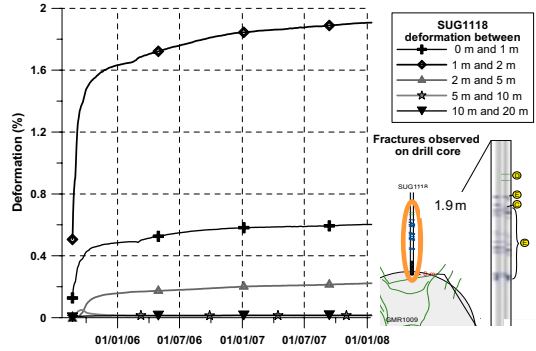


Fig. 3. Deformation measured in the vertical borehole (SUG1118) at the vault in the SMR1.1 (parallel to σ_h)

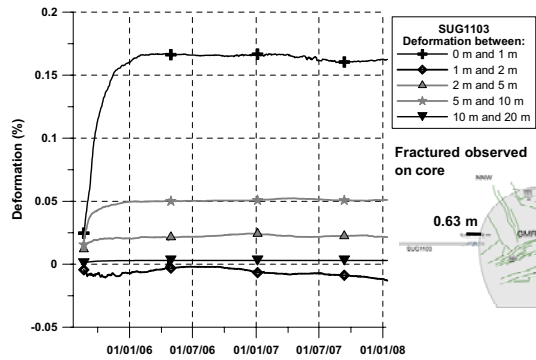


Fig. 4. Deformation measured in the horizontal borehole SUG1103 at the wall in the SMR1.1 (parallel to σ_h)

3 CONSTITUTIVE EQUATIONS

The short-term behaviour is based on the constitutive model used by Andra in the framework of the European project: EURATOM MODEX-REP (Su, 2003) and modified by Souley et al. (2003). The main features of this model are: (a) linear elasticity for modelling the phase I (in pre-peak behaviour); (b) damage initiation and growth (phase II in pre peak) are approached by a strain-hardening based on Hoek-Brown criterion. Hoek-Brown constants (m , s) and uniaxial compressive strength (σ_c) are used to define the two independent internal variables A and B depending upon plastic strain ($A = m \sigma_c$, $B = s \sigma_c^2$); (c) the peak, post-peak (phase III) and residual phase (phase VI) are also based on Hoek-Brown criterion with respect to brittle/ductile transition in accordance with the experimental data.

The generalized Hoek-Brown yield function is used for damage, failure and residual behaviour. The general form of the yield function (including the three principal stresses and the stress geometry through the Lode's angle, θ) is expressed in the following equation:

$$F(p, q, \theta) = -\frac{\chi}{\sigma_3^{b-d}} \left[p + q \left(\frac{\cos \theta}{\sqrt{3}} - \frac{\sin \theta}{3} \right) \right] + \frac{2}{\sqrt{3}} q \cos \theta - \chi - \sqrt{-A \left[p + q \left(\frac{\cos \theta}{\sqrt{3}} - \frac{\sin \theta}{3} \right) \right] + B} \quad (1)$$

where χ : softening flow function (parabolic form with respect to the internal plastic variable or plastic distortion γ in phase III, and null elsewhere); p : mean effective stress; q : generalized deviatoric stress; σ_3^{b-d} : confining pressure leading to brittle/ductile transition and

depending on the post-peak strength parameters. A and B linearly vary with γ in phase II (from the onset of damage defined by: m^{end} , s^{end} , σ_c^{end} to the peak defined by: m^{rup} , s^{rup} , σ_c^{rup}), and remain constant in phase III and IV.

In the literature only few examples (see synthesis in Clausen & Damkilde 2008) of implementation of Hoek-Brown criterion in numerical codes are given and these implementations are generally based on rounding the corner and the apex, except the work of Clausen & Damkilde (2008). These authors develop an algorithm for generalized Hoek-Brown criterion including the apex and corner singularities. As the yield function $F(p, q, \theta)$ and its first derivatives are not defined and continuous everywhere in the stress space, Eq. (1) is extended as follows:

$$F_s(p, q, \theta) = \frac{\left\{ \frac{\chi}{\sigma_3^{b-d}} \left[p + q \left(\frac{\cos \theta}{\sqrt{3}} - \frac{\sin \theta}{3} \right) \right] - \frac{2}{\sqrt{3}} q \cos \theta + \chi \right\}^2}{A} + p + q \left(\frac{\cos \theta}{\sqrt{3}} - \frac{\sin \theta}{3} \right) - \frac{B}{A} \quad (2)$$

In addition to $F_s(p, q, \theta)$ and its first (and more) derivatives are continuous everywhere in stress space, it is not necessary to re-evaluate Hoek-Brown parameters (at the onset of damage and at failure) already determined by overall analysis of sample tests.

For long-term behaviour, a creep model is proposed on the basis of the main observations made during the creep tests (Su, 2003): (a) creep strain rate accelerates non-linearly as deviatoric stress increases; (b) creep strain rate varies as a function of viscoplastic strain; the analysis of those variables suggests a strain-hardening function based on a power law; (c) the trend of the creep strain rate to increase non-linearly with temperature may be expressed by Arrhenius law decreasing exponentially; (d) a creep threshold of 3 to 5 MPa may be the case beyond which creep may take place. For practical applications, the deviatoric stress threshold can be chosen on the basis of the natural in situ stress state (p_0, q_0) and the difference between the natural stress state and the induced ones (p, q), according:

$$g(p, q) = \exp\left(-\left((q - q_0)^2 + (p - p_0)^2\right)^{\frac{\varpi}{2}}\right) \quad (3)$$

where ϖ is a constant indicating the velocity to which one reaches the threshold of the natural stress state (p_0, q_0) from a stress state strongly modified in the vicinity of openings.

By taking all these phenomena into account, the following expression was proposed for viscoplastic strain rate tensor:

$$\underline{\underline{\dot{\varepsilon}}}^{vp} = A_0(T) \exp\left(-\frac{B}{RT}\right) \left(\frac{q - q_0 g(p, q)}{\sigma_0}\right)^n (\underline{\underline{\varepsilon}}_{eq}^{vp})^m \frac{\partial q}{\partial \underline{\underline{\sigma}}} \quad (4)$$

where B: activation energy; R: Boltzmann constant; T: absolute temperature; A_0 : intact material viscosity at a reference temperature; σ_0 : reference stress; n: dimensionless exponent traducing the deviatoric stress power factor; m: exponent of hardening work;

$\underline{\underline{\varepsilon}}_{eq}^{vp} = \sqrt{\frac{2}{3} \underline{\underline{\varepsilon}}^{vp} : \underline{\underline{\varepsilon}}^{vp}}$: viscoplastic strain (or viscoplastic distortion in accordance with the observed negligible volumetric strains during creep tests).

In situ observations thus highlighted the influence of damage on the creep strain rate. In the same way, when the deviatoric stress reaches a certain value between 15 and 18 MPa, the

creep tests also show that Lemaître's model (with parameters identified from the tests with stress level lower than 15 MPa) under-estimates the strains. These observations lead us to express the influence of the damage on the viscoplastic strain rate through one or several following forms: (a) the exponent n of deviatoric stress; (b) the activation energy; (c) the hardening power factor. Due to fact that deviatoric stress is rather related to the loading history (its increase making the damage growth), we firstly privileged to vary the hardening exponent and the energy of activation with respect to the damage state.

Let m_0 and m_1 ($0 > m_0 \geq m_1$) be respectively the hardening parameter corresponding to the intact (undamaged) and broken (post-failure state: from peak to the residual phase) materials. In absence of experimental data, we propose an evolution of the damaged material exponent m between m_0 and m_1 which supposes slow hardening exponent rates around these two states:

$$m = m(\gamma) = 2(m_0 - m_1)(\gamma^*)^3 - 3(m_0 - m_1)(\gamma^*)^2 + m_0 \quad (5)$$

$\gamma^* = \min(\gamma / \gamma^{rup}, 1)$: where γ and γ^{rup} are the current and peak value of shear plastic strain (plastic distortion).

If we postulate that influence of damage on creep activation energy can be approached by an exponential function: $\exp(b_1 \gamma^*)$, then the proposed model for viscoplastic strain rate is expressed:

$$\underline{\underline{\dot{\varepsilon}}}^{vp} = A_0(T) \exp\left(-\frac{B}{RT} + b_1 \gamma^*\right) \left(\frac{q - q_0 \sqrt{(q - q_0)^2 + (p - p_0)^2}}{\sigma_0}\right)^n (\varepsilon_{eq}^{vp})^{m(\gamma^*)} \frac{\partial q}{\partial \underline{\underline{\sigma}}} \quad (6)$$

Assuming that only small strains occurred (justified by low strain rates measured in situ for a period of 2 years as reported by Gasc et al., 2004), total strain increment, $d\underline{\underline{\varepsilon}}$, can be subdivided into instantaneous elastic strains, $d\underline{\underline{\varepsilon}}^e$; instantaneous plastic strains (or damaged/plastic strains since damage is herein approached by theory of plasticity), $d\underline{\underline{\varepsilon}}^p$; and time-dependent creep strain $d\underline{\underline{\varepsilon}}^{vp}$ (evaluated from the viscoplastic strain rate tensor in Eq. 6). Assuming an associated flow rule (for simplicity), the damaged/plastic strain increment is given by:

$$d\underline{\underline{\varepsilon}}^p = \lambda \frac{\partial G}{\partial \underline{\underline{\sigma}}} = \lambda \frac{\partial F_s}{\partial \underline{\underline{\sigma}}} \quad (7)$$

$$d\gamma = \lambda \frac{\partial F_s}{\partial q} = \sqrt{\frac{2}{3}} d\underline{\underline{e}}^p : d\underline{\underline{e}}^p = \sqrt{\frac{2}{3}} d e_{ij}^p e_{ij}^p \quad \text{with} \quad d\underline{\underline{e}}^p = d\underline{\underline{\varepsilon}}^p - \frac{tr(d\underline{\underline{\varepsilon}}^p)}{3} \underline{\underline{\delta}} \quad (8)$$

where λ : plastic multiplier determined from the consistency condition $dF_s(\underline{\underline{\sigma}}, \gamma) = 0$. This allows to express the stress increment as a function of total and viscoplastic strain increments through the fourth order elastic compliance tensor $\underline{\underline{\underline{C}}}$:

$$d\underline{\underline{\sigma}} = \left[\begin{array}{c} \left(\underline{\underline{C}} : \frac{\partial \underline{\underline{F}}_s}{\partial \underline{\underline{\sigma}}} \right) \otimes \left(\underline{\underline{C}} : \frac{\partial \underline{\underline{F}}_s}{\partial \underline{\underline{\sigma}}} \right) \\ \underline{\underline{C}} - \frac{\frac{\partial \underline{\underline{F}}_s}{\partial \underline{\underline{\sigma}}} : \underline{\underline{C}} : \frac{\partial \underline{\underline{F}}_s}{\partial \underline{\underline{\sigma}}} - \frac{\partial \underline{\underline{F}}_s}{\partial \gamma} \frac{\partial \underline{\underline{F}}_s}{\partial q}}{\underline{\underline{C}}} \end{array} \right] : (d\underline{\underline{\varepsilon}} - d\underline{\underline{\varepsilon}}^{vp}) \quad (9)$$

Except for the m_1 and b_1 , all the other parameters were already identified either from creep tests on intact material or from triaxial tests for the short-term response (Su, 2003). Since only the results of two creep tests are available with deviatoric stress close to the peak (say on damaged materials), the constants m_1 and b_1 are back-evaluated from the observed in situ convergences. Typical values of the model input parameters are summarized in Table 1: (a) elastic properties: E , ν ; (b) onset on damage parameters: m^{end} , s^{end} , σ_c^{end} ; (c) peak strength parameters: m^{rup} , s^{rup} , σ_c^{rup} ; (d) residual strength parameters: α , β ; (e) parameters for time-dependent behaviour of intact material: A_0 , B , n , m_0 ; (f) parameters for time-dependent behaviour of broken material: m_1 , b_1 .

Contrary to the recent formulation of Zhou et al. (2008), we do not take into account the explicit influence of viscoplasticity on plasticity since the authors consider total plastic deformation as the sum of instantaneous plastic strain and delayed plastic strain. Moreover, without data, the influence of viscosity on long-term strength of the argillites is not taken into account in this model, even if the induced damage may be responsible for the material failure and the strength decreases when the loading rate decreases.

Table 1. Typical mean values of short-term and long-term behaviour corresponding to the main level of -490 m at LS/MHM laboratory

m^{end}	s^{end}	σ_c^{end} (MPa)	m^{rup}	s^{rup}	σ_c^{rup} (MPa)
0.9	1	15	2.5	0.43	33.5

α	β (MPa)	γ^{rup}	γ^{res}	E (MPa)	ν
3.3	3	0.00575	0.0155	5600	0.3

A_0 (h^{-1})	B (J mol^{-1})	n	m_0	m_1	b_1
$1.158 \cdot 10^{-14}$	63000	6.8	-2.7	-5.75	1.6

4 NUMERICAL IMPLEMENTATION AND VERIFICATION

4.1 Numerical implementation

In the three-dimensional explicit finite-difference code, *FLAC*^{3D}®, we have implemented the model coupling the damage state with viscoplastic strain rate, as described above. At each creep time-step, Eq. (6) and (9) are solved using Crank-Nicolson method and a central-difference formulation.

4.2 Verification

In order to verify the short-term part of the implemented model, seven triaxial compression tests with confining pressures of 2, 5, 10, 12, 16, 20 and 25 MPa are simulated. They are a part of the wide number of triaxial compression tests characterizing the non-linear behaviour of the studied materials. The resulting curves (not presented in this paper) display four regions (elastic, damage in pre-peak, softening in post-peak and residual phase) when the confining pressure is below the transition stress level $\sigma_3^{\text{b-d}}$, and three regions (elastic, damage

and perfect plastic phase) under high confining pressure. In addition, the onset of damage (limit between elastic/damage region), the peak and residual strengths derived from these simulations are compared with the theoretical envelopes: the corresponding relative error does not exceed 0.3%.

The proposed model is applied to simulate relaxation tests performed on argillites for a confining pressure of 10 MPa and available in Su, (2003). The evolutions of deviatoric stress in time for the four tests are recalled in Fig. 5. The numerical simulation carried out with the proposed model is also shown in Fig. 5. Due to the deviatoric stress reached before the relaxation is lower than the onset of damage (approximately 20 MPa for 10 MPa of confining pressure, the sample remains undamaged. Qualitatively, the model response is in agreement with the curves provided by laboratory tests. From a quantitative point of view, the model is perfectly in agreement with the results of test E5083_7 and E5171_4 as well on the loading rate at the beginning of tests, as on the plateau of deviatoric stress near 8 MPa.

Fig. 6 illustrates a simulation of a relaxation test for 3 different total axial strain levels. As observed from laboratory relaxation tests, one notices that relaxation becomes faster and more important when the strain increases.

Fig. 7 shows the effect of damage on viscoplastic strains from the simulations of triaxial multi-stage creep tests for a confining pressure of about 10 MPa. In the first simulation (without effect of damage), it was assumed that both undamaged and broken materials behave similarly: $m_1=m_0$; $b_1=0$). At the first stage, since the onset of damage is not reached, the evolution of viscoplastic distortion remains identical. The two last stages correspond to two different levels of material damage: 30 and 70% of maximum damage prior to the failure (peak). It should be noticed when the damage rate is high, the viscoplastic strains become increasingly large.

The proposed model was used to predict the radial creep of an infinitely long, cylindrical cavity in a rock mass subjected to an isotropic stress state. Assuming that creep is defined by steady-state a single-component power law ($\dot{\epsilon}_{eq}^{vp} = A q^r$), the analytical steady-state solution is provided by van Sambeek (1986). This solution is used to validate the proposed model when both damage and its influence on the viscoplastic strains are ignored.

For this problem, $A=10^{-9}$ MPa⁻³ yr⁻¹; $r=3$. The appropriated model input parameters are considered and the onset of damage is set to infinite in order to preserve damage development. The initial isotropic stress is about -20 MPa.

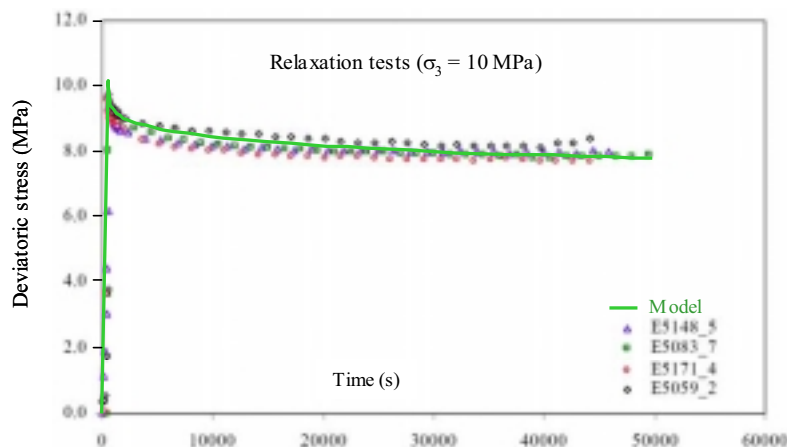


Fig. 5. Simulation of relaxation test using the proposed model : comparison with the laboratory tests

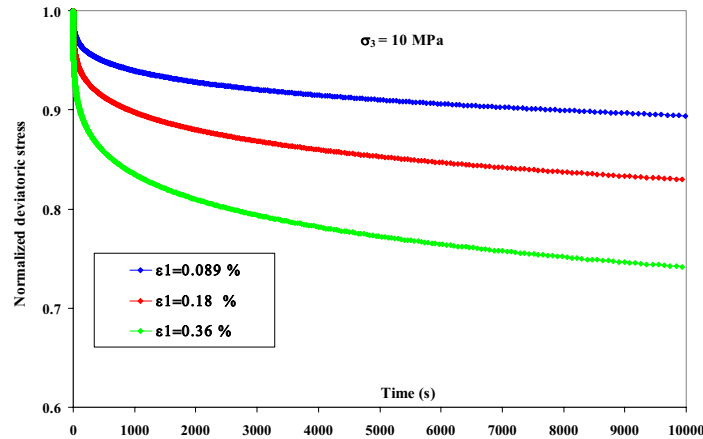


Fig. 6. Simulation of relaxation test per stage ($\sigma_3 = 10$ MPa) at three levels of deviatoric stress ($q = \sigma_1 - \sigma_3$): $q = 5$ MPa ($\varepsilon_1 = 0.089\%$), $q = 10$ MPa ($\varepsilon_1 = 0.18\%$) et $q = 25$ MPa ($\varepsilon_1 = 0.36\%$)

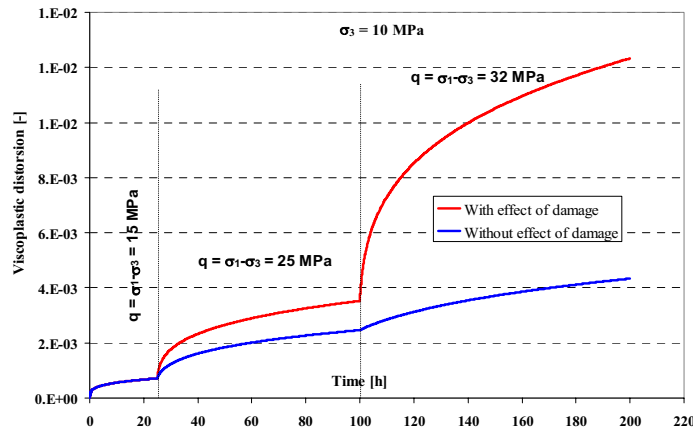


Fig. 7. Viscoplastic shear strain for a multi-stage creep test simulation (1st stage $q = 15$ MPa; 2nd stage $q = 25$ MPa and 3rd stage $q = 32$ MPa)

Fig. 8 shows the evolution of radial and orthoradial stresses (compressive stresses are negative) with respect to the radial distance from the cavity wall. Comparison between the model and the analytical solution indicates a good agreement since the relative error is lower than 0.3 %.

For the same example, the influence of damage on the creep behaviour is investigated. In this case, appropriate parameters for damage, peak and residual strength are used (Table 1). The effect of damage on the viscoplastic strains is activated through the activation energy (b_1) since both m_0 and m_1 remain null. Fig. 9 shows the evolution of radial and orthoradial stresses where damage impacts the amplitudes of the stresses in comparison to the viscoelastic solution. In addition, the presence of damage leads to increase the viscoplastic strain rates (not presented here): this comes up to our expectations. Compared with viscoelastic solution, the damage contributes to increase the amplitude of radial displacement velocity from $0.62 \cdot 10^{-5}$ to $1.7 \cdot 10^{-5}$ m/y at the cavity wall.

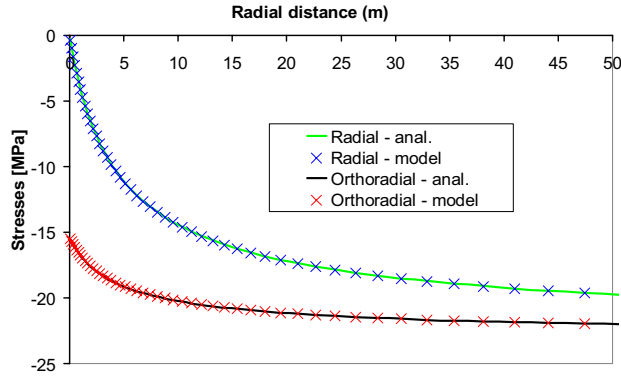


Fig. 8. Comparison of radial and orthoradial stresses at steady-state: continue (analytical solution); cross (proposed model: $A_0=1.9e-2 \text{ h}^{-1}$; $n=3$; $m_0=m_1=-1e-20$; $b_1=0$)

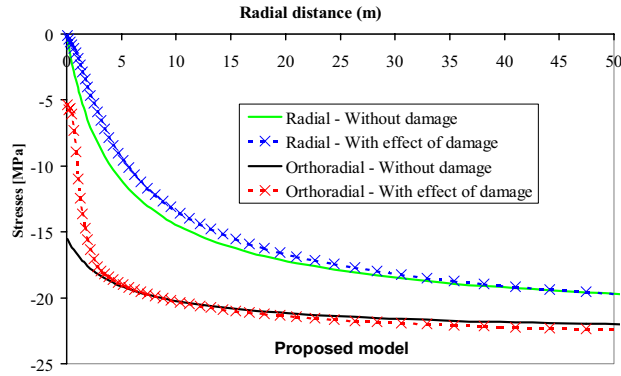


Fig. 9. Comparison of radial and orthoradial stresses at steady-state: continue ($A_0=1.9e-2 \text{ h}^{-1}$; $n=3$; $m_0=m_1=-1e-20$; $b_1=0$); cross ($A_0=1.9e-2 \text{ h}^{-1}$; $n=3$; $m_0=m_1=-1e-20$; $b_1=1.6$)

5 CONCLUSIONS

This paper presented the development of a model for long-term behaviour of Callovo-Oxfordian argillites. The model integrates the deformations measured in laboratory and corresponding to those observed in situ. Also the impact of the damaged and fractured zones in cavities near field upon viscoplastic deformations amplitudes is considered in a simplified and pragmatic manner using hardening flow and activation energy.

The model is developed from experimental considerations, based on laboratory characterization as well as in situ evidences of damage influence on viscoplastic strains. More precisely, it generalizes two rheological models developed in the framework of MODEX-REP European project : one for the short-term response in which damage is approached by plasticity theory using the criterion of Hoek-Brown; the other for the long-term behaviour according to the modified Lemaître's model. The changes of viscoplastic strain rates due to damage are herein taken into account by varying the creep activation energy and the strain-hardening as a function of the current damage rate. Other approaches, in particular, phenomenological micromechanics are currently under study by several teams with the objectives to understand the mechanisms related to creep acceleration due to induced damage and to develop models behaviour.

The proposed macroscopic model is implemented in the three-dimensional code *FLAC^{3D}*. Simulations of triaxial compression tests at different confining pressures provide a verification of the implemented model, in particular, by comparing the predicted damage threshold, peak and residual strengths profiles with the theoretical ones.

The simulation of laboratory relaxation tests allows to confirm that the proposed model is relevant since the input parameters of the time-dependent behaviour are derived only from creep tests. The model prediction is in agreement with the measurements and the results of Shao et al., (2003).

The influence of damage on the creep behaviour was highlighted by simulating a multi-stage creep test and by comparing the viscoplastic deformation according to whether the sample remains intact or damaged. This influence was also shown in the simulation (1D) of a cylindrical cavity excavated in a viscoplastic medium.

As practical applications, in a paper accompanying this one, we used the proposed model for predictive calculations of two galleries of the laboratory LS/MHM (at -490 m level): parallel and perpendicular to the major horizontal stress.

REFERENCES

- Armand, G., Nussbaum, C, Cruchaudet, M. and Rebours, H. (2009) Characterisation of the Excavated Damaged Zone (EDZ) in the Meuse Haute-Marne underground research laboratory, *In Proceedings of the International Conference on Rock Joints and Jointed Rock Masses*, January 4-9 ,2009 , TUCSON, USA
- Armand, G., Wileveau, Y., Morel, J., Cruchaudet, M. and Rebours, H. (2007) Excavated Damaged Zone (EDZ) in the Meuse Haute-Marne underground research laboratory, *In Proceedings of the 11th congress of the ISRM, Lisbon, Portugal*, 9-13 July 2007, Eds. L. Ribeiro e Sousa, C. Olalla and N. Grossmann, 33-36
- Clausen, J. and Damkilde L. (2008), “An exact implementation of the Hoek–Brown criterion for elasto-plastic finite element calculations”, *Int J Rock Mech Min Sci* 45(6), 831–847
- Gasc-Barbier, M., Chanchole, S. & Bérest, P. (2004), “Creep behaviour of Bure clayey rock”, *Appl. Clay Sci.*, 26(20), 449-458
- Shao, J.F., Zhu, Q.Z. & Su, K. (2003), “Modeling of creep in rock materials in terms of material degradation”, *Computers and Geotechnics*, Vol.30, 549-555
- Souley, M., Su, K., Ghoreychi, M. and Armand, G. (2003), “Constitutive models for rock mass : numerical implementation, verification and validation” in *FLAC and Numerical Modeling in Geomechanics*, Brummer et al. (eds), ISBN 90 5809 581 9
- Su, K. (2003), Constitutive Models for the Meuse/Haute-Marne Argillites – MODEX-REP, European Commission – Nuclear science and technology, Contract n° FIKW-CT2000-00029, Deliverable 2-3.
- Van Sambeek, L. L. (1986), “Creep of Rock Salt under Inhomogeneous Stress Conditions” Ph.D. Thesis, Colorado School of Mines
- Wileveau, Y., Renaud, V., Kazmierczak, J.-B. and Armand, G. (2006) Rheological characterization of a clay formation from drifts excavation: elastic and elastoplastic approach, *In Proceeding of Sea to Sky Geotechnique 2006*, Vancouver, Canada, 1-4 October 2006.
- Zhou, H., Jia, Y. & Shao, J.F. (2008), “A unified elastic–plastic and viscoplastic damage model for quasi-brittle rocks”. *Int. J. Rock. Mech. Min. Sci.*, Vol. 45(8), 1237-1251.